

Spectral splits of neutrinos as a BCS-BEC crossover type phenomenon

Y. Pehlivan,^{1,*} A. L. Subaşı,² N. Ghazanfari,¹ S. Birol,³ and H. Yüksel¹

¹*Department of Physics, Mimar Sinan Fine Arts University, Sisli, Istanbul, 34380, Turkey*

²*Department of Physics, Istanbul Technical University, Istanbul, Turkey*

³*Department of Physics, Istanbul University, Istanbul, Turkey*

(Dated: February 1, 2022)

We show that the spectral split of a neutrino ensemble which initially consists of electron type neutrinos, is analogous to the BCS-BEC crossover already observed in ultra cold atomic gas experiments. Such a neutrino ensemble mimics the deleptonization burst of a core collapse supernova. Although these two phenomena belong to very different domains of physics, the propagation of neutrinos from highly interacting inner regions of the supernova to the vacuum is reminiscent of the evolution of Cooper pairs between weak and strong interaction regimes during the crossover. The Hamiltonians and the corresponding many-body states undergo very similar transformations if one replaces the pair quasispin of the latter with the neutrino isospin of the former.

PACS numbers: 14.60.Pq, 67.85.-d, 74.20.Fg, 95.85.Ry, 97.60.Bw.

Keywords: BCS-BEC crossover, Collective neutrino oscillations, neutrino spectral splits, supernova.

I. INTRODUCTION

A core-collapse supernova releases 99% of its energy in the form of neutrinos in the MeV energy scale [1, 2]. Our basic understanding about these neutrinos was confirmed [3, 4] when supernova 1987A exploded in our neighbor galaxy, the Large Magellanic Cloud, and generated 19 neutrino events in Kamiokande [5] and IBM [6] detectors. The next important breakthrough in this field will be the observation of neutrinos from a supernova explosion in our own galaxy which is estimated to generate thousands of neutrino events in current neutrino detectors [7]. Therefore a future galactic supernova presents a unique opportunity to test our understanding of neutrinos. This includes the many-body aspects of their flavor transformations [8, 9] which develop via the neutrino-neutrino ($\nu\nu$) interactions in the supernova [10, 11].

Although neutrino cross sections are extremely small, their tiny scattering amplitudes can add up coherently to give rise to a finite effect when neutrinos propagate in the presence of a matter background [12]. This is similar to the refraction of light in matter except that, since neutrinos can interact with each other via neutral current, they can also create a *self refraction* effect on themselves [11]. Two kinds of diagrams, shown in Fig. 1, add up coherently in self refraction: (a) the forward scattering diagram in which there is no momentum transfer between particles and (b) the exchange diagram in which particles completely swap their momenta [8, 9]. The former gives rise to an ordinary refraction index through the optical theorem [12]. The latter can be viewed as a *flavor-exchange* diagram between neutrinos and, as such, it couples the flavor transformation of each neutrino to the flavor content of the entire neutrino ensemble. This turns the flavor evolution of neutrinos near the core of a

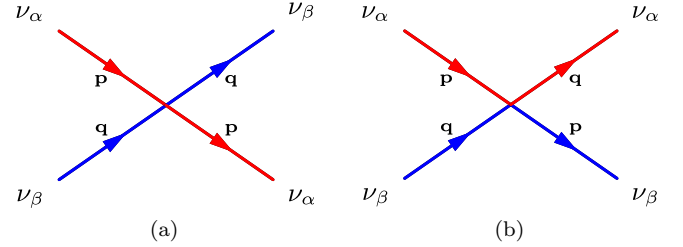


FIG. 1. (Color online) Forward (a) and exchange (b) diagrams which add up coherently in $\nu\nu$ scattering.

supernova into a many-body problem [13–18].

The correlations between flavor histories of neutrinos with different energies, which are referred to as *collective neutrino oscillations*, have been extensively studied [19–26]. The large array of resulting nonlinear and emergent behavior displayed by self interacting neutrinos are reminiscent of condensed matter systems. A formal analogy between collective neutrino oscillations and BCS pairing model of superconductivity [27] has recently been pointed out by Pehlivan *et al.* [15, 16] and further elaborated in [28]. Besides the Cooper pairs of electrons in superconductors, BCS pairing is observed in a broad range of many body systems, including neutron stars and atomic nuclei [29], ultra cold atomic gases [30, 31] and excitonic condensates in semiconductor structures [32–34].

One collective behavior observed in some numerical simulations of neutrinos emerging from supernova is the *spectral split* or *spectral swap* phenomenon in which neutrinos in different flavor (or mass) eigenstates completely exchange their spectra around a certain critical energy [22, 24]. In this paper we show that, for a neutrino ensemble which initially consists of only electron type neutrinos, the formation of the spectral split also corresponds to the well known BCS-BEC crossover [35, 36] phenomenon. We describe the neutrinos using the effective two flavor mixing scenario and the neutrino bulb

* yamac.pehlivan@msgsu.edu.tr

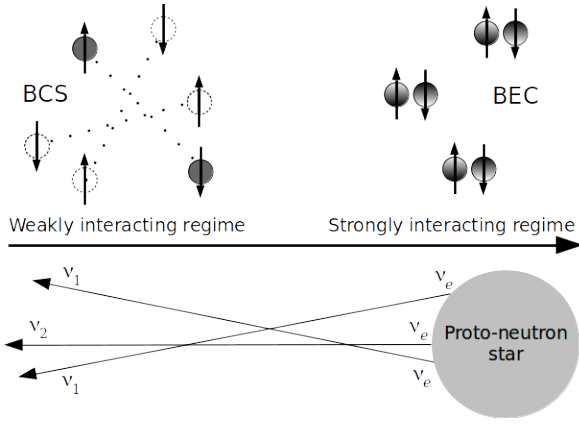


FIG. 2. The correspondence between self interacting neutrinos in a core collapse supernova and BCS-BEC crossover. Neutrinos are emitted by the proto-neutrino star which forms at the center after the core collapse. Just outside the surface of the proto-neutrino star, neutrino self interaction rate is very high which corresponds to the BEC limit. As the neutrinos move away from the center, the interaction rate decreases and approaches the BCS limit.

model under the mean field approximation. Such a model can be considered as an heuristic description of the initial deleptonization phase of a core collapse supernova. We illustrate BCS-BEC crossover correspondence in ultra cold atomic gases which have been used to simulate other quantum systems as in creation of Dirac monopoles and observation of quantum phase transitions [37, 38] and make analogies with different physical phenomena like black hole evaporation and cosmological effects [39–42]. The correspondence considered here doesn't imply any pairing correlations between the neutrinos. As illustrated in Fig. 2, it is a more subtle analogy in which the electron neutrinos originally released by the proto-neutrino star at the center are identified with the quasi-hole pairs of the BEC (spheres with graded color) whereas the first and second neutrino mass eigenstates far from the center are identified with the real hole (empty spheres) and particle (solid black spheres) pairs, respectively.

This paper is organized as follows: in Section II, we briefly review the analogy between BCS pairing Hamiltonian and the self interacting neutrinos. In Section III, we introduce the analogy between BCS-BEC crossover in cold atoms and the neutrino spectral split. We discuss our results and conclude in Section IV.

II. BCS PAIRS AND SELF INTERACTING NEUTRINOS

The BCS model describes the superconducting state of weakly interacting fermions through a coherent superposition of Cooper pairs. In ultra cold dilute gas systems, the pairing interaction between fermionic atoms can be

described by the mean-field Hamiltonian

$$H_{\text{BCS}} = \sum_k \begin{pmatrix} c_{k\uparrow}^\dagger & c_{\bar{k}\downarrow} \end{pmatrix} \begin{pmatrix} \epsilon_k - \mu & -g\Delta^- \\ -g\Delta^+ & -\epsilon_k + \mu \end{pmatrix} \begin{pmatrix} c_{k\uparrow} \\ c_{\bar{k}\downarrow}^\dagger \end{pmatrix}. \quad (1)$$

We assume that the atoms can occupy a discrete set of energy levels ϵ_k and the operators $c_{k\uparrow}$ and $c_{\bar{k}\downarrow}$ annihilate spin-up and spin-down fermions, respectively, in the k^{th} time-reversed energy levels. The chemical potential μ is introduced as a Lagrange multiplier to fix the average particle number. The interactions can be tuned via Feshbach resonances [43] which function as a control knob for the coupling constant g . The physics is captured by the mean field

$$\vec{\Delta} = \left(\frac{\Delta^+ + \Delta^-}{2}, \frac{\Delta^+ - \Delta^-}{2i}, \Delta^0 \right) \quad (2)$$

where

$$\Delta^- = \sum_\ell \langle c_{\bar{\ell}\downarrow} c_{\ell\uparrow} \rangle, \quad \Delta^0 = \sum_\ell \left\langle \frac{c_{\ell\uparrow}^\dagger c_{\ell\uparrow} - c_{\bar{\ell}\downarrow}^\dagger c_{\bar{\ell}\downarrow}}{2} \right\rangle. \quad (3)$$

The pairing potential $\Delta^- = (\Delta^+)^*$ describes the scattering of zero center-of-mass momentum pairs and Δ^0 corresponds to the Hartree potential which can be included in the definition of μ , i.e., $\mu \rightarrow \mu + g\Delta^0$. In Eq. (3), the expectation values are calculated with respect to a state which satisfies the usual mean field self-consistency requirements.

The flavor evolution of self interacting neutrinos near the core of a supernova is described by a mathematically similar Hamiltonian

$$H_{\nu\nu} = \frac{1}{2} \sum_k \begin{pmatrix} a_{k2}^\dagger & a_{k1}^\dagger \end{pmatrix} \begin{pmatrix} -\omega_k + \lambda & GP^- \\ GP^+ & \omega_k - \lambda \end{pmatrix} \begin{pmatrix} a_{k2} \\ a_{k1} \end{pmatrix}. \quad (4)$$

We assume that neutrinos are box quantized in volume V and therefore occupy a discrete set of energy levels ε_k . The operator a_{ki} annihilates a neutrino in the k^{th} energy level, in the mass eigenstate with mass m_i ($i = 1, 2$). To be specific, we assume that $m_1 > m_2$ which corresponds to inverted mass hierarchy. The oscillation frequency for a neutrino with energy ε_k associated with this mass difference is given by

$$\omega_k = (m_1^2 - m_2^2)/2\varepsilon_k. \quad (5)$$

The Lagrange multiplier λ plays an analogous role to the chemical potential μ in Eq. (1) as discussed in Ref. [15]. $\nu\nu$ interaction strength is given by

$$G = \frac{2\sqrt{2}G_F}{V} D(r) \quad (6)$$

where the Fermi constant G_F appears due to our use of the Fermi 4-point interaction as shown in Fig. 1. We also use the neutrino bulb model which approximates the angular dependence of the $\nu\nu$ scattering amplitude [44] with an effective geometrical factor $D(r) \propto 1/r^2$ [22] where r is the distance from the supernova center. Combined with decreasing neutrino density which increases the normal-

ization volume, G drops as $1/r^4$.

Here, we adopt an effective two flavor mixing scenario

$$a_{ke} = \cos \vartheta a_{k1} + \sin \vartheta a_{k2}, \quad a_{k\mu} = \sin \vartheta a_{k1} - \cos \vartheta a_{k2}, \quad (7)$$

where the effects of the third flavor and the other background particles are absorbed in a single mixing angle ϑ and a single mass squared difference (see e.g. [14, 45]). In Eq. (4), $\nu\nu$ interactions are described by the mean field \vec{P} defined by

$$P^- = \sum_{\ell} \langle a_{\ell 1}^{\dagger} a_{\ell 2} \rangle \quad P^0 = \sum_{\ell} \left\langle \frac{a_{\ell 2}^{\dagger} a_{\ell 2} - a_{\ell 1}^{\dagger} a_{\ell 1}}{2} \right\rangle. \quad (8)$$

The components P^{\pm} create the exchange diagrams shown in Fig. 1b while P^0 creates the forward scattering diagram in Fig. 1a. P^0 contributes to the diagonal of Eq. (4) and plays a similar role to that of an Hartree potential for fermionic pairs. In the case of neutrinos, P^0 is always non-zero, and we include it in the definition of λ in order to highlight the resemblance with the BCS model.

The similarity between Eqs. (1) and (4) suggests the mapping

$$a_{k2} \leftrightarrow c_{k\uparrow} \quad \text{and} \quad a_{k1} \leftrightarrow c_{k\downarrow}^{\dagger}, \quad (9)$$

which reveals the common $SU(2)$ group structure of these problems. This group is generated by the *quasispin operators* for BCS pairs [46] given by

$$J_k^- = c_{k\downarrow} c_{k\uparrow} \quad J_k^0 = \frac{1}{2} (c_{k\uparrow}^{\dagger} c_{k\uparrow} - c_{k\downarrow}^{\dagger} c_{k\downarrow}), \quad (10)$$

and the *mass isospin operators* for neutrinos given by

$$J_k^- = a_{k1}^{\dagger} a_{k2} \quad J_k^0 = \frac{1}{2} (a_{k2}^{\dagger} a_{k2} - a_{k1}^{\dagger} a_{k1}). \quad (11)$$

For convenience, we denote both the pair quasispin and the neutrino isospin with the same symbol but it is always clear which one is being referred to from the context. In both cases, components of \vec{J}_k obey the $SU(2)$ algebra, i.e.,

$$[J_k^+, J_{\ell}^-] = 2\delta_{k\ell} J_k^0, \quad \text{and} \quad [J_k^0, J_{\ell}^{\pm}] = \pm\delta_{k\ell} J_k^{\pm}. \quad (12)$$

In terms of these operators, the Hamiltonians describing the BCS pairs and self interacting neutrinos can be written respectively as

$$H_{\text{BCS}} = \sum_k 2(\epsilon_k - \mu) J_k^0 - g \left(\langle J^- \rangle J^+ + \langle J^+ \rangle J^- \right) \\ H_{\nu\nu} = - \sum_k (\omega_k - \lambda) J_k^0 + \frac{G}{2} \left(\langle J^- \rangle J^+ + \langle J^+ \rangle J^- \right) \quad (13)$$

where \vec{J} is the total quasi-/iso-spin operator for all energy levels, i.e., $\vec{J} = \sum_k \vec{J}_k$. Note that the two Hamiltonians differ by an overall minus sign.

Eq. (10) tells us that for a single energy level k , quasispin up and down states correspond to that level being occupied ($|\uparrow\downarrow\rangle$) or unoccupied ($|\text{---}\rangle$) by a pair, respectively. (Levels occupied by unpaired atoms decouple

Self interacting neutrinos		Fermions with pairing	
Mass eigenstates	$ \nu_1\rangle$ $ \nu_2\rangle$	$ \text{---}\rangle$ $ \uparrow\downarrow\rangle$	Pair states
Neutrino operators in mass basis	a_{1k}^{\dagger} a_{2k}^{\dagger}	$c_{k\downarrow}$ $c_{k\uparrow}^{\dagger}$	Particle-hole operators
Neutrino operators in flavor basis	a_{ek}^{\dagger} $a_{\mu k}^{\dagger}$	$\lim_{g \rightarrow \infty} \tilde{c}_{k\downarrow}$ $\lim_{g \rightarrow \infty} \tilde{c}_{k\uparrow}^{\dagger}$	Quasi particle- hole operators

TABLE I. The analogous states and operators in the correspondence between the self interacting neutrinos and BCS pairing.

from the pairing dynamics and are ignored here.) In the case of neutrinos, Eq. (11) tells us that the isospin up and down states for energy level k correspond to the neutrino occupying that energy level being in ν_2 and ν_1 mass eigenstate, respectively. Therefore, the analogous states are

$$|\uparrow\downarrow\rangle \leftrightarrow |\nu_2\rangle \quad \text{and} \quad |\text{---}\rangle \leftrightarrow |\nu_1\rangle. \quad (14)$$

Considering all the energy levels in the system, the state in which all neutrinos are in the ν_1 mass eigenstate corresponds to the *particle vacuum* of the BCS model, i.e., the state with no pairs in it:

$$|\emptyset\rangle \equiv |\text{---} \text{---} \text{---} \dots\rangle \leftrightarrow |\nu_1 \nu_1 \nu_1 \dots\rangle. \quad (15)$$

Clearly the particle vacuum of the BCS model has no dynamics but neither does the neutrino state on the right hand side of Eq. (15): since all the neutrinos are in mass eigenstate, this state does not undergo vacuum oscillations and since all the neutrinos are in the same mass eigenstate, exchange diagrams shown in Fig. 1b cannot change this state either. Acting on both states in Eq. (15) with J_k^+ repeatedly, we find

$$|\uparrow\downarrow \text{---} \text{---} \dots\rangle \leftrightarrow |\nu_2 \nu_1 \nu_1 \nu_1 \dots\rangle, \\ |\uparrow\downarrow \uparrow\downarrow \text{---} \text{---} \dots\rangle \leftrightarrow |\nu_2 \nu_2 \nu_1 \nu_1 \dots\rangle, \quad (16)$$

and so on. The pairs on the left now scatter between the energy levels while the neutrinos on the right undergo exchange interactions.

III. BCS-BEC CROSSOVER AND SPECTRAL SPLITS

The ground state of the pairing Hamiltonian evolves from weakly bound Cooper pairs in the BCS limit of vanishing interactions to the Bose-Einstein condensation of tightly bound diatomic molecules in the limit of strong interactions. This evolution takes place without a phase

Self interacting neutrinos		Fermions with pairing	
Oscillation frequency	ω_k	$2\epsilon_k$	Pair energy
Split frequency	ω_c	$2\epsilon_F$	Fermi energy
Lagrange multiplier	λ	2μ	Chem. potential
Interaction strength	G	$2g$	Pairing strength
Neutrino mean field	P^\pm	Δ^\pm	Pair mean field
Neutrino numbers in mass eigenstates	$\frac{n_1(k) - n_2(k)}{2}$	$n_p(k) - \frac{1}{2}$	Pair occupation number

TABLE II. The list of analogous scalar quantities in the correspondence between the self interacting neutrinos and BCS pairing. The last two lines follow from the analogy between pair quasispin and neutrino isospin, i.e., Eqs. (10) and (11). Here $n_i(k)$ is the number of neutrinos in the eigenstate with mass m_i in the k^{th} energy mode and $n_p(k)$ is the number of pairs in the k^{th} energy level.

transition as the interaction strength is varied and hence the ground state can be described by the same variational BCS wave function throughout the crossover between BCS and BEC limits [47, 48]. The theoretical prediction has been experimentally observed in ultra cold atomic systems [49–53].

The variational BCS ground state of the Hamiltonian in Eq. (1) can be written as

$$\begin{aligned}
 |\text{BCS}\rangle &= \prod_k \left(\cos \theta_k + \sin \theta_k c_{k\uparrow}^\dagger c_{k\downarrow}^\dagger \right) |\emptyset\rangle \\
 &= \prod_k (\cos \theta_k |-\rangle_k + \sin \theta_k |\uparrow\downarrow\rangle_k)
 \end{aligned} \quad (17)$$

where the angle θ_k is to be found from

$$\cos 2\theta_k = \frac{(\epsilon_k - \mu)}{E_k} \quad (18)$$

with

$$E_k = \sqrt{(\epsilon_k - \mu)^2 + g^2 \Delta^+ \Delta^-}. \quad (19)$$

The requirement that the state in Eq. (17) should satisfy Eq. (3) gives rise to the self-consistency equations

$$\begin{aligned}
 \frac{1}{g} &= \sum_k \frac{f_k - \frac{1}{2}}{E_k}, \\
 \sum_k \left(n_p(k) - \frac{1}{2} \right) &= \sum_k \frac{\epsilon_k - \mu}{E_k} \left(f_k - \frac{1}{2} \right)
 \end{aligned} \quad (20)$$

which determine the mean field Δ^\pm and the chemical potential μ . The distribution of the quasiparticles is given

by the Fermi function

$$f_k = \frac{1}{\exp(E_k/k_B T) + 1} \quad (21)$$

where T is the temperature and k_B is the Boltzmann constant. It is also useful to define the quasiparticle operators

$$\tilde{c}_{k\uparrow} = \cos \theta_k c_{k\uparrow} - \sin \theta_k c_{k\downarrow}^\dagger, \quad \tilde{c}_{k\downarrow} = \sin \theta_k c_{k\uparrow}^\dagger + \cos \theta_k c_{k\downarrow}, \quad (22)$$

which annihilate the BCS ground state so that $|\text{BCS}\rangle$ can be viewed as a quasiparticle vacuum. Accordingly, pair occupation numbers in the $|\text{BCS}\rangle$ state are given by

$$n_p(k) = \langle c_{k\uparrow}^\dagger c_{k\uparrow} \rangle = \langle c_{k\downarrow}^\dagger c_{k\downarrow} \rangle = \sin^2 \theta_k. \quad (23)$$

These occupation numbers can be calculated for any value of the interaction constant g by first solving the self consistency equations given in Eq. (20) for the mean field Δ^\pm and chemical potential μ , and then calculating θ_k from Eqs. (18) and (19).

In the weak interaction limit, the solution describes the non-interacting Fermi sea with

$$\lim_{g \rightarrow 0} \theta_k = \frac{\pi}{2} \Theta(\epsilon_F - \epsilon_k) \quad (24)$$

where $\Theta(x)$ denotes the Heaviside step function and

$$\lim_{g \rightarrow 0} \mu = \epsilon_F \quad (25)$$

is the Fermi energy. Fig. 3a shows the corresponding particle (blue dashed line) and hole (red dotted line) occupation numbers in this limit which follow from substituting Eq. (24) in Eq. (23). The particle pairs fill the levels up to the Fermi energy and the system displays the characteristic distribution of a degenerate ideal Fermi gas at zero temperature.

The interaction strength increases from left to right in the upper panel of Fig. 3 and the distributions are gradually smoothed out as more and more levels start to take part in pairing. In the limit of strong interactions the angle θ_k tends to the same value for all pairs, i.e.,

$$\lim_{g \rightarrow \infty} \theta_k = \theta. \quad (26)$$

In this limit, $|\text{BCS}\rangle$ represents a BEC in the form of a coherent state of atomic pairs occupying the same single-pair quantum state. Fig. 3d displays the occupation numbers of particle and hole pairs which are almost uniform in this limit indicating that all levels are taking part in pairing. Here, quasihole distribution is also shown with a solid black line. Note that the quasihole distribution is equal to unity and remains the same throughout the crossover for any value of g because $|\text{BCS}\rangle$ is the quasiparticle vacuum, but it is indicated only in this plot to emphasize its resemblance to the ν_e distribution in the strong neutrino self interaction regime (see below).

The typical evolution of the chemical potential in the BCS-BEC crossover from positive values to negative values is shown in the left panel of Fig. 4 as a function of

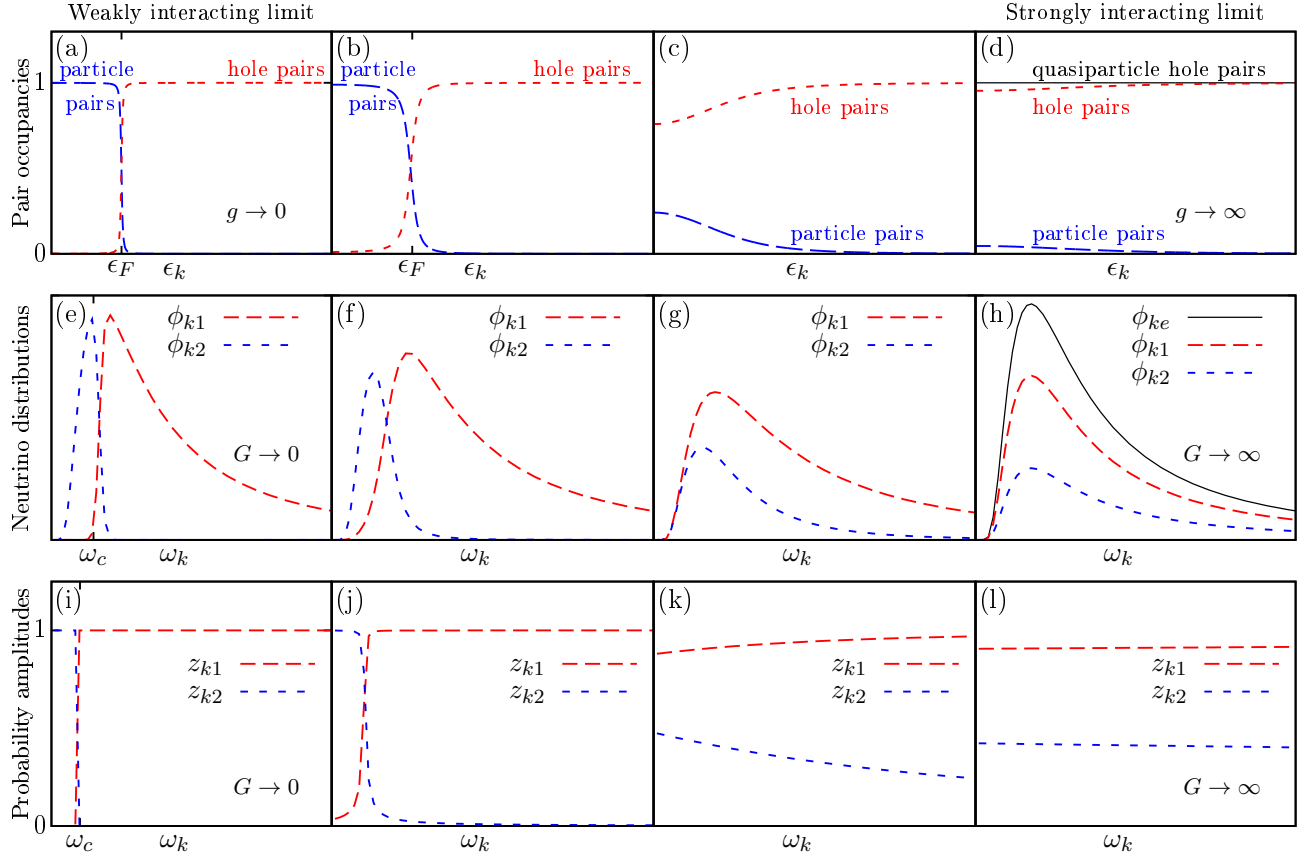


FIG. 3. (Color online) *Upper panel:* Evolution of pair distributions as the interaction strength increases from left to right. (a) and (d) show the weakly (BCS) and strongly (BEC) interacting limits of BCS-BEC crossover, respectively. *Middle panel:* Evolution of neutrino distributions as the neutrinos move away from the supernova core (strongly interacting regime) to the outer layers (weakly interacting regime) from right to left. (h) shows the assumed ν_e distribution near the supernova core which is normalized to 1, as well as the corresponding ν_1 and ν_2 distributions. As the neutrinos evolve from strong to weak interaction regime, a spectral split develops as shown on (e). *Lower panel:* Evolution of the probability amplitudes z_{1k} and z_{2k} , of finding a neutrino in the first and second mass eigenstates, respectively.

the inverse scattering length, the parameter characterizing the strength of the pairing interaction. The vanishing of the chemical potential is accompanied with the shift of excitation energy minimum to zero momentum and is identified as the separation point between the BCS and BEC sides of the crossover.

For self interacting neutrinos, the state which is analogous to $|\text{BCS}\rangle$ can be written down using Table I:

$$|\text{“BCS”}\rangle = \prod_k \left(\cos \theta_k + \sin \theta_k a_{k2}^\dagger a_{k1} \right) |\nu_1 \nu_1 \nu_1 \dots\rangle \\ = \prod_k (\cos \theta_k |\nu_1\rangle_k + \sin \theta_k |\nu_2\rangle_k) \quad (27)$$

Here, the angle θ_k and the associated self consistency equations are the same as those given in Eqs. (18-20) with the replacements shown in Table (II) and $f_k - 1/2 \rightarrow -\phi_e/2$ where ϕ_e is the Fermi function describing electron neutrino energy distribution. The last replacement follows from the analogy between pair quasispin and neutrino isospin (see Eqs. (10) and (11)). Due to the overall

sign difference between the two Hamiltonians given in Eq. (13), $|\text{“BCS”}\rangle$ is not the ground state of the neutrino Hamiltonian, but its highest energy eigenstate. However, since the energy spectra of the two Hamiltonians are the same apart from an overall sign, $|\text{“BCS”}\rangle$ should also evolve smoothly between strong and weak interaction regimes without a phase transition (i.e., with no level crossings).

Using Eq. (9), one can also define the analogs of the quasiparticle operators introduced in Eq. (22)

$$\tilde{a}_{k2} = \cos \theta_k a_{k2} - \sin \theta_k a_{k1}, \quad \tilde{a}_{k1}^\dagger = \sin \theta_k a_{k2}^\dagger + \cos \theta_k a_{k1}^\dagger, \quad (28)$$

which similarly annihilate the $|\text{“BCS”}\rangle$ state. Note that, unlike the operators in Eq. (22), these operators do not mix particle and hole states which is consistent with the number conserving nature of the neutrino self interactions. Denoting the states associated with the operators \tilde{a}_1^\dagger and \tilde{a}_2^\dagger by $|\tilde{\nu}_1\rangle$ and $|\tilde{\nu}_2\rangle$, respectively, this tells us that the $|\text{“BCS”}\rangle$ state is a $|\tilde{\nu}_1\rangle$ condensate.

For neutrinos, the limit of strong self interactions is

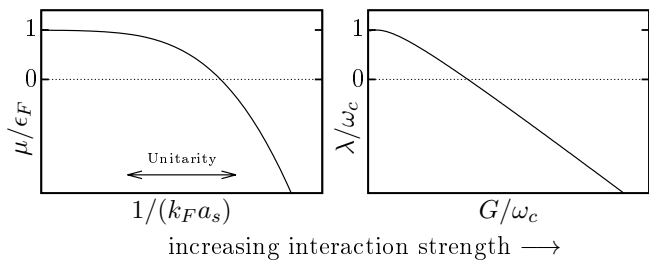


FIG. 4. *Left panel:* Chemical potential μ calculated from Eqs. (3) vs. the scattering length a_s characterizing the interactions. (ϵ_F/k_F denotes the Fermi energy/momentum.) *Right panel:* Lagrange multiplier λ calculated from Eqs. (8) vs. the interaction parameter G . ($\omega_c = \lim_{G \rightarrow 0} \lambda$) For both panels, the analogous parameters g and G increase from left to right. $\mu = 0$ and $\lambda = 0$ are the boundary points between BCS and BEC regimes.

realized near the core of the supernova. In general, the flavor composition of neutrinos released from the core depends on the explosion phase. Here we consider a special case in which all neutrinos are released as ν_e , which is more relevant for the initial stages of the explosion. For such a configuration, the solution of the consistency equations given in Eq. (8) yield

$$\lim_{G \rightarrow \infty} \theta_k = \vartheta \quad (29)$$

where ϑ is the neutrino mixing angle introduced in Eq. (7). This is similar to the BEC regime of the fermion pairs. Substituting this angle in Eq. (27) and using Eq. (7) gives

$$|\text{“BCS”}\rangle = |\nu_e \nu_e \nu_e \dots\rangle \quad (30)$$

which confirms the self-consistency of the state. In this limit, the quasiparticle operators which annihilate this state become the particle operators in flavor basis, i.e.,

$$\tilde{a}_{k2} = a_{k\mu} \quad \text{and} \quad \tilde{a}_{k1}^\dagger = a_{k\epsilon}^\dagger. \quad (31)$$

In Fig. 3h, we plot neutrino occupation numbers associated with the |“BCS”⟩ state in this limit. Note that, although the pairing Hamiltonian in Eq. (1) describes the atomic pairs at ultra low temperatures, the Hamiltonian in Eq. (4) represents self interactions of neutrinos for any (thermal or non-thermal) energy distribution. The main features of the analogy is independent of the neutrino energy distribution. For illustration, we use a thermal ν_e distribution with a temperature of 5 MeV which is shown with the solid-black line. The corresponding ν_1 and ν_2 occupation numbers which follow from Eq. (7) are shown with red-dotted and blue-dashed lines, respectively.

As the neutrinos move away from the core of the supernova, $\nu\nu$ interactions are gradually turned off as described by Eq. (6). Therefore, one expects the |“BCS”⟩ state to evolve in a way which is similar to the BCS-BEC crossover of |BCS⟩ state, but reversed in the direction of decreasing interaction strength. The middle panel of

Fig. 3 shows the evolution of the neutrino distributions as the neutrino self interaction constant G decreases from *right to left*. In the dilute, weakly interacting regime where

$$\lim_{G \rightarrow 0} \lambda = \omega_c, \quad (32)$$

the state |“BCS”⟩ in Eq. (27) evolves into

$$|\text{“BCS”}\rangle = \prod_{\omega_k < \omega_c} |\nu_2\rangle_k \prod_{\omega_k > \omega_c} |\nu_1\rangle_k \quad (33)$$

under the adiabatic evolution conditions. This distribution is plotted in Fig. 3e and corresponds to the BCS limit of the fermion pairing. This is a particular example of a *spectral split* phenomenon, so called because the original ν_e energy distribution is eventually split between the two mass eigenstates. This phenomenon was observed in numerical simulations of supernova neutrinos by various groups (see Refs. [24, 25] for review).

The similarity between pair distribution of cold atoms which we treat at zero temperature, and the neutrino distribution which we treat at finite temperature becomes pronounced if we focus on the *Bogoliubov coefficients*

$$z_{k1} = \frac{\langle a_{k1}^\dagger \tilde{a}_{k1} \rangle}{\langle \tilde{a}_{k1}^\dagger \tilde{a}_{k1} \rangle} = \cos \theta_k, \quad z_{k2} = \frac{\langle a_{k2}^\dagger \tilde{a}_{k1} \rangle}{\langle \tilde{a}_{k1}^\dagger \tilde{a}_{k1} \rangle} = \sin \theta_k. \quad (34)$$

These are the probability amplitudes for the neutrino born in the state $|\nu_e\rangle$ near the core (where it almost overlaps with $|\tilde{\nu}_1\rangle$) to be found in $|\nu_1\rangle$ or $|\nu_2\rangle$ mass eigenstate, respectively. The evolutions of these coefficients are shown in the lower panel of Fig. 3 as a function of the interaction constant. In strongly interacting limit near the center of the supernova Bogoliubov coefficients are uniform with $z_{k1} \rightarrow \cos \vartheta$ and $z_{k2} \rightarrow \sin \vartheta$ but as the neutrinos move away from the center, $|\tilde{\nu}_1\rangle$ becomes more and more like $|\nu_2\rangle$ (or $|\nu_1\rangle$) for low (high) ω values. This is reminiscent of the fact that, during the BCS-BEC crossover, quasihole degrees of freedom at the BEC limit coincide with real particles (holes) for low (high) energies at the BCS limit.

In Fig. 5, we plot the eigenvalues of the fermion pairing (left panel) and self interacting neutrino (right panel) Hamiltonians for three representative values of the respective interaction strengths. For the fermion pairs, these eigenvalues are $\pm E_k$ with E_k given by Eq. (19). For neutrinos, they are given by the same formula with the replacements from Table II. The solid black lines represent the weakly interacting limits where the chemical potential μ and the Lagrange multiplier λ almost coincide with their limiting values which are the Fermi energy ϵ_F , and the split frequency ω_c , respectively. The dashed blue lines correspond to the point at which μ and λ become zero, and the dotted red lines represent the regime in which they are negative. In the case of fermion pairs, the difference between these eigenvalues ($2E_k$) is the energy gap for the creation of a quasiparticle pair excitation in the system. This energy gap is minimized at $\epsilon_k = \mu$ on the BCS side, i.e. while $\mu > 0$, and at $\epsilon_k = 0$ on the BEC

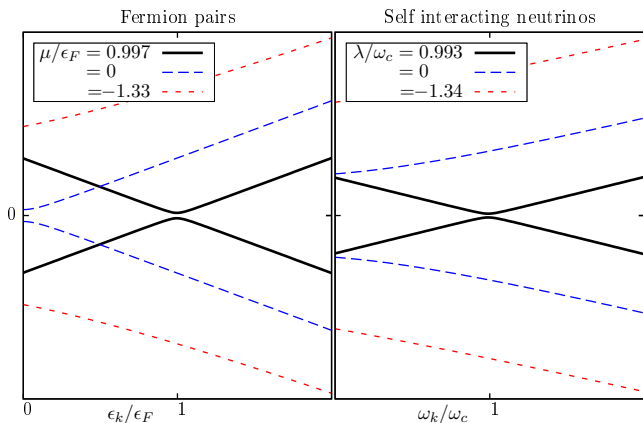


FIG. 5. *Left panel:* Eigenvalues of the Hamiltonian matrix for fermion pairs given in Eq. (1) at three different values of the interaction constant g corresponding to three different values of the chemical potential. $\mu/\epsilon_F = 1$ (solid black line) is on the BCS limit, $\mu/\epsilon_F < 0$ is on BEC side (red dotted line), and $\mu = 0$ (blue dashed line) is the boundary between BCS and BEC regimes. *Right panel:* Eigenvalues of the Hamiltonian matrix for self interacting neutrinos given in Eq. (4) for three different values of the interaction constant G corresponding to positive, zero, and negative values of the Lagrange multiplier λ . $\lambda = 0$ is the boundary between BCS and BEC regimes.

side, i.e. while $\mu < 0$. As a result, as the interaction constant increases, the location of the minimum moves from the Fermi surface to the zero momentum. Therefore, the excitations from the BCS groundstate are always gapped. In the case of neutrinos, the difference $2E_k$ is the energy gap between the states $|\tilde{\nu}_1\rangle$ and $|\tilde{\nu}_2\rangle$, which leads to the avoided level crossing in this model. It is minimized for neutrinos with oscillation frequency $\omega_k = \lambda$ while $\lambda > 0$ and $\omega_k = 0$ while $\lambda < 0$. Near the core of the supernova where self interactions dominate, this minimum is located at $\omega_k = 0$. As the interaction strength decreases, the minimum gap moves until it eventually reaches to ω_c .

For the cold atoms, the shifting of the location of the minimum gap to zero momentum with increasing g occurs when $\mu = 0$ which indicates that the system has moved from BCS to BEC side. For the neutrinos, although G decreases as they move away from the supernova core, the energy distributions initially do not change significantly. The change begins soon after the location of the minimum gap moves to $\omega = 0$ which occurs when $\lambda = 0$. Therefore, the fact that the minimum gap coincides with $\omega = 0$ can be seen as the beginning of the split phenomenon.

IV. SUMMARY & CONCLUSIONS

We showed an analogy between the spectral split of a neutrino ensemble which initially consists of electron type neutrinos, and the BCS-BEC crossover phenomenon. This analogy is illustrated using the BCS model of ultra

cold atomic gases. Due to their mathematically equivalent Hamiltonians, these systems undergo identical transformations while they evolve from strong to weak interaction regimes. In particular, the Fermi energy of the BCS model and the critical split frequency of neutrinos play analogous roles. Note that although the pair quasispin and the neutrino isospin obey the same algebra, the latter is number conserving whereas the former is not. As a result, in Eqs. (15-16), BCS pair states live in a Fock space whereas the neutrino states live in a regular Hilbert space. The energy gap plotted in Fig. 5 is a quasipair excitation gap in the case of cold atoms from the ground state, whereas for neutrinos, it is the energy difference between the two mixing eigenstates.

In the BEC limit, all atomic pairs occupy the same state so that the configuration is maximally symmetric. The analog neutrino state should also be maximally symmetric, i.e., all neutrinos should initially have the same flavor. We choose that to be ν_e to associate the initial state with the neutralization burst of supernova, but any other flavor could have been chosen. Antineutrinos of the opposite flavor ($\bar{\nu}_\mu$ in our case) could also be added to the picture without breaking the analogy because neutrinos and antineutrinos transform under the conjugate representations, e.g., $\bar{\nu}_\mu$ transforms in the same way as ν_e . In other words, the BCS-BEC crossover analogy considered here would hold for any maximally symmetric initial state which consists of neutrinos of one type, and antineutrinos of the opposite type. For such a state, the split occurs in the neutrino sector and the behavior of antineutrinos is dictated by the *lepton number conservation*, i.e., the conservation of P^0 defined in Eq. (8) ([22, 54]). Other neutrino spectral split scenarios involving less symmetric initial configurations, do not correspond to a simple BCS-BEC crossover. Such initial neutrino states may display more complicated behavior including multiple spectral splits [55]. It is an open question whether or not these splits correspond to some other phenomena in the fermion pairing scheme.

In a realistic supernova setting small quantities of non-electron flavor neutrinos would be present in the initial deleptonization phase. Moreover, recent simulations suggest that the neutrino spectral splits are unstable against the inclusion of the multi angle and three flavor effects [23, 56], both of which are important in a real supernova but are omitted in this study. Still, the present analogy can be helpful in understanding some aspects of collective flavor oscillations in supernova. For example, an experimental cold atom system can be used to *simulate* the possible contribution of entangled many-body states to the collective behaviour of neutrinos [15–17, 57, 58]. Such a contribution will present itself as a deviation of the experimental cold atom system from the results obtained by the mean field approximation which is currently employed by most numerical studies of supernova neutrinos, including the one presented here. Possible departures from adiabaticity [59], the factors affecting the split frequency [60–62], and even the multi angle

instability of split behavior mentioned above can be subjects of such an experimental study. Moreover, in the full three flavor mixing case neutrino isospin generalizes to an $SU(3)$ operator [16]. There are pairing scenarios for atomic systems [63, 64] and in QCD [65] suggesting similar analogies in this case. A possible extension of our analogy in this direction may help us to gain insight about the three flavor instability.

Finally, other quantum many-body systems, in which the relative strength of kinetic and interaction energies is density dependent, might also have been considered in lieu of ultra cold atomic Fermi gases in our discussion.

For instance, in the context of excitonic condensates, the BCS-BEC crossover is driven by density [66]. In such electronic systems with long range Coulomb interactions, somewhat counter-intuitively, the low density limit results in a strongly interacting system. For neutrinos, the self interaction term is density dependent because many scattering amplitudes must coherently superpose to generate the effect. Thus, unlike the case of excitonic condensates, the relative strength of neutrino self interactions decreases with density.

Y.P. thanks to CETUP* 2015 organizers for allowing a stimulating environment. This work was supported by TÜBİTAK under project number 115F214.

-
- [1] S. A. Colgate and R. H. White, *Astrophys.J.* **143**, 626 (1966).
 - [2] S. Woosley and T. Weaver, *Ann.Rev.Astron.Astrophys.* **24**, 205 (1986).
 - [3] W. D. Arnett, J. N. Bahcall, R. P. Kirshner, and S. E. Woosley, *Ann. Rev. Astron. Astrophys.* **27**, 629 (1989).
 - [4] A. Burrows and J. M. Lattimer, *Astrophys.J.* **318**, L63 (1987).
 - [5] K. Hirata *et al.* (KAMIOKANDE-II Collaboration), *Phys.Rev.Lett.* **58**, 1490 (1987).
 - [6] R. Bionta, G. Blewitt, C. Bratton, D. Casper, A. Ciocio, *et al.*, *Phys.Rev.Lett.* **58**, 1494 (1987).
 - [7] K. Scholberg, *Ann.Rev.Nucl.Part.Sci.* **62**, 81 (2012).
 - [8] J. T. Pantaleone, *Phys.Rev.* **D46**, 510 (1992).
 - [9] J. T. Pantaleone, *Phys.Lett.* **B287**, 128 (1992).
 - [10] D. Yu. Bardin, S. M. Bilenky, and B. Pontecorvo, *Phys. Lett.* **B32**, 121 (1970).
 - [11] G. M. Fuller, R. W. Mayle, J. R. Wilson, and D. N. Schramm, *Astrophys.J.* **322**, 795 (1987).
 - [12] L. Wolfenstein, *Phys.Rev.* **D17**, 2369 (1978).
 - [13] R. F. Sawyer, *Phys.Rev.* **D72**, 045003 (2005).
 - [14] A. B. Balantekin and Y. Pehlivan, *J.Phys.* **G34**, 47 (2007).
 - [15] Y. Pehlivan, A. B. Balantekin, T. Kajino, and T. Yoshida, *Phys.Rev.* **D84**, 065008 (2011).
 - [16] Y. Pehlivan, A. B. Balantekin, and T. Kajino, *Phys.Rev.* **D90**, 065011 (2014).
 - [17] C. Volpe, D. Väänänen, and C. Espinoza, *Phys. Rev.* **D87**, 113010 (2013).
 - [18] J. Serreau and C. Volpe, *Phys.Rev.* **D90**, 125040 (2014).
 - [19] S. Samuel, *Phys.Rev.* **D48**, 1462 (1993).
 - [20] V. A. Kostelecky and S. Samuel, *Phys.Rev.* **D52**, 621 (1995).
 - [21] S. Samuel, *Phys.Rev.* **D53**, 5382 (1996).
 - [22] H. Duan, G. M. Fuller, J. Carlson, and Y.-Z. Qian, *Phys.Rev.* **D74**, 105014 (2006).
 - [23] A. Friedland, *Phys.Rev.Lett.* **104**, 191102 (2010).
 - [24] H. Duan, G. M. Fuller, and Y.-Z. Qian, *Ann.Rev.Nucl.Part.Sci.* **60**, 569 (2010).
 - [25] A. Mirizzi, I. Tamborra, H.-T. Janka, N. Saviano, K. Scholberg, R. Bollig, L. Hudepohl, and S. Chakraborty, *Riv. Nuovo Cim.* **39**, 1 (2016).
 - [26] S. Chakraborty, R. Hansen, I. Izaguirre, and G. Raffelt, *Nucl. Phys.* **B908**, 366 (2016).
 - [27] J. Bardeen, L. Cooper, and J. Schrieffer, *Phys.Rev.* **108**, 1175 (1957).
 - [28] T. E. Baker, *ArXiv e-prints* (2016), arXiv:1601.00913 [hep-ph].
 - [29] D. J. Dean and M. Hjorth-Jensen, *Rev. Mod. Phys.* **75**, 607 (2003).
 - [30] I. Bloch, J. Dalibard, and W. Zwerger, *Rev. Mod. Phys.* **80**, 885 (2008).
 - [31] S. Giorgini, L. P. Pitaevskii, and S. Stringari, *Rev. Mod. Phys.* **80**, 1215 (2008).
 - [32] X. Zhu, P. B. Littlewood, M. S. Hybertsen, and T. M. Rice, *Phys. Rev. Lett.* **74**, 1633 (1995).
 - [33] J. Keeling, P. R. Eastham, M. H. Szymanska, and P. B. Littlewood, *Phys. Rev. B* **72**, 115320 (2005).
 - [34] T. Byrnes, N. Y. Kim, and Y. Yamamoto, *Nat. Phys.* **10**, 803 (2014).
 - [35] M. W. Zwierlein, in *Novel Superfluids: Volume 2*, edited by K.-H. Bennemann and J. B. Ketterson (Oxford Scientific Publications, Oxford, 2014) Chap. 18, p. 269.
 - [36] M. Randeria and E. Taylor, *Annual Review of Condensed Matter Physics* **5**, 209 (2014).
 - [37] M. W. Ray, E. Ruokokoski, S. Kandel, M. Möttönen, and D. S. Hall, *Nature* **505**, 657 (2014).
 - [38] M. Greiner, O. Mandel, T. Esslinger, T. W. Hansch, and I. Bloch, *Nature* **415**, 39 (2002).
 - [39] L. J. Garay, J. R. Anglin, J. I. Cirac, and P. Zoller, *Phys. Rev. Lett.* **85**, 4643 (2000).
 - [40] S. Giovanazzi, *Phys. Rev. Lett.* **94**, 061302 (2005).
 - [41] J.-C. Jaskula, G. B. Partridge, M. Bonneau, R. Lopes, J. Ruaudel, D. Boiron, and C. I. Westbrook, *Phys. Rev. Lett.* **109**, 220401 (2012).
 - [42] C.-L. Hung, V. Gurarie, and C. Chin, *Science* **341**, 1213 (2013).
 - [43] S. Inouye, M. R. Andrews, J. Stenger, H.-J. Miesner, D. M. Stamper-Kurn, and W. Ketterle, *Nature* **392**, 151 (1998).
 - [44] G. Sigl and G. Raffelt, *Nucl.Phys.* **B406**, 423 (1993).
 - [45] T.-K. Kuo and J. T. Pantaleone, *Rev.Mod.Phys.* **61**, 937 (1989).
 - [46] P. W. Anderson, *Phys. Rev.* **112**, 1900 (1958).
 - [47] D. M. Eagles, *Phys. Rev.* **186**, 456 (1969).
 - [48] A. J. Leggett, in *Modern Trends in the Theory of Condensed Matter*, edited by A. Pekalski and R. Przystawa (Springer-Verlag, Berlin, 1980) pp. 13–27.

- [49] C. A. Regal, M. Greiner, and D. S. Jin, Phys. Rev. Lett. **92**, 040403 (2004).
- [50] M. Bartenstein, A. Altmeyer, S. Riedl, S. Jochim, C. Chin, J. H. Denschlag, and R. Grimm, Phys. Rev. Lett. **92**, 120401 (2004).
- [51] M. W. Zwierlein, C. A. Stan, C. H. Schunck, S. M. F. Raupach, A. J. Kerman, and W. Ketterle, Phys. Rev. Lett. **92**, 120403 (2004).
- [52] J. Kinast, S. L. Hemmer, M. E. Gehm, A. Turlapov, and J. E. Thomas, Phys. Rev. Lett. **92**, 150402 (2004).
- [53] T. Bourdel, L. Khaykovich, J. Cubizolles, J. Zhang, F. Chevy, M. Teichmann, L. Tarruell, S. J. J. M. F. Kokkelmans, and C. Salomon, Phys. Rev. Lett. **93**, 050401 (2004).
- [54] G. L. Fogli, E. Lisi, A. Marrone, and A. Mirizzi, JCAP **0712**, 010 (2007), arXiv:0707.1998 [hep-ph].
- [55] B. Dasgupta, A. Dighe, G. G. Raffelt, and A. Yu. Smirnov, Phys. Rev. Lett. **103**, 051105 (2009), arXiv:0904.3542 [hep-ph].
- [56] G. Raffelt, S. Sarikas, and D. de Sousa Seixas, Phys. Rev. Lett. **111**, 091101 (2013).
- [57] A. Friedland and C. Lunardini, Phys. Rev. **D68**, 013007 (2003).
- [58] A. Friedland and C. Lunardini, JHEP **0310**, 043 (2003).
- [59] B. Dasgupta, A. Mirizzi, I. Tamborra, and R. Tomas, Phys. Rev. **D81**, 093008 (2010).
- [60] G. Fogli, E. Lisi, A. Marrone, and I. Tamborra, JCAP **0910**, 002 (2009).
- [61] S. Sarikas, D. de S. Seixas, and G. Raffelt, Phys. Rev. **D86**, 125020 (2012).
- [62] G. G. Raffelt, Phys. Rev. **D83**, 105022 (2011).
- [63] C. Honerkamp and W. Hofstetter, Phys. Rev. B **70**, 094521 (2004).
- [64] P. F. Bedaque and J. P. D’Incao, Annals of Physics **324**, 1763 (2009).
- [65] M. G. Alford, A. Schmitt, K. Rajagopal, and T. Schäfer, Rev. Mod. Phys. **80**, 1455 (2008).
- [66] N. Andrenacci, A. Perali, P. Pieri, and G. C. Strinati, Phys. Rev. B **60**, 12410 (1999).